Research Article

NMR IN BIOMEDICINE

Received: 16 April 2008, Revised: 22 January 2009, Accepted: 22 January 2009, Published online in Wiley InterScience: 2009

(www.interscience.wiley.com) DOI:10.1002/nbm.1377

^{1}H HR-MAS and genomic analysis of human tumor biopsies discriminate between high and low grade astrocytomas

Valeria Righi[a,b,c], Jose M. Roda[d], José Paz[d], Adele Mucci[b], Vitaliano Tugnoli[c], Gemma Rodriguez-Tarduchy[a], Laura Barrios[e], Luisa Schenetti[b], Sebastián Cerdán[a]* and María L. García-Martín[a,†]

We investigate the profile of choline metabolites and the expression of the genes of the Kennedy pathway in biopsies of human gliomas ($n = 23$) using ^{1}H High Resolution Magic Angle Spinning (HR-MAS, 11.7 Tesla, 277 K, 4000 Hz) and individual genetic assays. ^{1}H HR-MAS spectra allowed the resolution and relative quantification by the LCModel of the resonances from choline (Cho), phosphocholine (PC) and glycerophosphorylcholine (GPC), the three main components of the combined tCho peak observed in gliomas by *in vivo* ^{1}H NMR spectroscopy. All glioma biopsies depicted a prominent tCho peak. However, the relative contributions of Cho, PC, and GPC to tCho were different for low and high grade gliomas. Whereas GPC is the main component in low grade gliomas, the high grade gliomas show a dominant contribution of PC. This circumstance allowed the discrimination of high and low grade gliomas by ^{1}H HR-MAS, a result that could not be obtained using the tCho/Cr ratio commonly used by *in vivo* ^{1}H NMR spectroscopy. The expression of the genes involved in choline metabolism has been investigated in the same biopsies. High grade gliomas depict an upregulation of the β gene of choline kinase and phospholipase C, as well as a downregulation of the cytidyltransferase B gene, the balance of these being consistent with the accumulation of PC. In the low grade gliomas, phospholipase A_1 and lysophospholypase are upregulated and phospholipase D is downregulated, supporting the accumulation of GPC. The present findings offer a promising procedure that will potentially help to accurately grade glioma tumors using ^{1}H HR-MAS, providing in addition the genetic background for the alterations of choline metabolism observed in high and low grade gliomas. Copyright © 2009 John Wiley & Sons, Ltd.

Keywords: choline metabolism; tumors; HR-MAS; gliomas; genomics

* *Correspondence to: S. Cerdán, Instituto de Investigaciones Biomédicas 'Alberto Sols' CSIC/UAM, c/ Arturo Duperier 4, Madrid 28029, Spain. E-mail: scerdan@iib.uam.es*

a *V. Righi, G. Rodriguez-Tarduchy, S. Cerdán, M. L. García-Martín Instituto de Investigationes Biomédicas 'Alberto Sols' CSIC/UAM, c/ Arturo Duperier 4, E-28029 Madrid, Spain*

b *V. Righi, A. Mucci, L. Schenetti Dipartimento di Chimica, Università di Modena, via G. Campi 183, I-41100 Modena, Italy*

c *V. Righi, V. Tugnoli Dipartimento di Biochimica 'G.Moruzzi', Università di Bologna, via Belmeloro 8/2, I- 40126 Bologna, Italy*

d *J. M. Roda, J. Paz Servicio de Neurocirurgia, Hospital Universitario 'La Paz', Madrid, Spain*

e *L. Barrios Centro Técnico de Informática CSIC, c/ Pinar 19, E-28006 Madrid, Spain*

† *Present address: RM Nuestra Señora del Rosario, c/ Principe de Vergara 53, Madrid 28012, Spain.*

Contract/grant sponsor: The Spanish Ministry of Education and Science; contract/grant numbers: SAF 2004–03197; NAN 2004–09125-C07–03.

Contract/grant sponsor: The Community of Madrid; contract/grant number: S-BIO/0179/2006.

Contract/grant sponsor: The Integrated EU Project MEDITRANS; contract/grant number: 026668.

Contract/grant sponsor: The Institute of Health Charles III; contract/grant number: PI051845.

Contract/grant sponsor: Italian Government; contract/grant number: IT0725H5F4.

Contract/grant sponsor: Acción Integrada Hispano-Italiana; contract/grant number: HI2006–0101.

Abbreviations used: *at, glycerol-3-phosphate acyltransferases (GPNAM); ck, choline kinase (CHKA, CHKB); ct, cytidylyl-transferase (PCYT1A, PCYT1B); CTL, choline transporter (CTL1, CTL2); COSY, COrrelation SpectroscopY; CPMG, Carr–Purcell–Meiboom–Gill; Cr/PCr, phosphocreatine; GABA, γ-amino butyric acid; Glu, glutamate; Glx, glutamine plus glutamate; GPC, glycerophosphocholine; GPE, glycerophosphorylethanolamine; HR-MAS, high-resolution magic angle spinning; Lac, lactate; Lip, lipids; lpl, lysophospholipase (LYPLA1); Man, mannitol; Myo, myo-inositol; NAA, N-acetylaspartate; pap, phosphatidate phosphohydrolase (PPAP2A); PC, phosphocholine; PE, phosphorylethanolamine; pla, phospholipase A (PLA2G6, PLA2G4A, PLA1A); plc, phospholipase C (PLCG1); pld, phospholipase D (PLD1, PLD2); ptc, phosphocholine cytidylyltransferase (CHPT1); Scy, scyllo-inositol; tCho, total choline; TOCSY, TOtal Correlation SpectroscopY.*

INTRODUCTION

Discrimination between high and low glioma grade remains a vital diagnostic decision, determining the most effective treatment and having an important impact on patient management and outcome (1–4). *In vivo* ^{1}H MR spectroscopic examinations are often used in clinical environments to assess tumor aggressiveness and help the MRI-based tumor diagnosis. A useful parameter in this sense is the total Choline (tCho) *versus* Creatine (Cr) ratio, which has previously been reported to be related to tumor grade (5–7). This diagnostic assigment has been helped more recently through the implementation of a variety of pattern recognition methodologies (8). The accuracy of these methods is increasing progressively, but difficulties remain currently in the unambiguous classification of high and low grade gliomas. This may be due to the fact that *in vivo* ^{1}H NMR spectroscopy approaches, as available in the clinic, are normally limited in sensitivity and resolution, resulting in relatively large voxel volumes and insufficient precission in the spectral assigments. In particular, the *in vivo* tCho peak, normally found to increase in high and low grade gliomas (9,10), contains contributions from a variety of choline containing metabolites including mainly, free choline (Cho), phosphocholine (PC), and glycerophosphocholine (GPC). In spite of the crucial information that these metabolites could provide on the alterations of phospholipid metabolism underlying transformation and progression of astrocytomas, their relative contribution to the combined Cho peak cannot be derived from the *in vivo* detected tCho resonance.

High Resolution Magic Angle Spinning (HR-MAS) approaches have been recently proposed to investigate normal and diseased tissues, thus overcoming some of the limitations of *in vivo* spectroscopy (11,12). The HR-MAS approach uses small biopsies of the tumors, providing similar sensitivity and resolution to that previously obtained from the high resolution ^{1}H NMR analyses of tumor extracts. However, few studies to date have investigated the metabolism of choline derivatives in human gliomas using this methodology (13,14).

Genomic approaches in tumors are currently envisioned to provide complementary information to the metabolic pattern obtained by HR-MAS, revealing the genomic 'finger print' of the tumor (15). In this respect, DNA microchips provide comprehensive information on complete genome expression but the analysis of the 57 000 genes dataset normally investigated is complex, and much of the information obtained is unrelated to the genes controlling choline transport and metabolism. The use of individual gene expression assays involving exclusively the genetic probes for the pathway of interest may provide a valuable alternative, reducing the complexity of the genomic analysis and facilitating a more focused interpretation.

In this work we hypothesized that HR-MAS could improve the performance of *in vivo* clinical ^{1}H NMR because of its enhanced resolution of the choline compounds and that analysis of the expression of choline metabolism genes could provide complementary information to interpret the observed HR-MAS alterations. Our results indicate that it is possible to discriminate between high grade and low grade gliomas on the basis of the choline metabolite profile as detected by HR-MAS and quantified with the LCModel program. The increased choline peak observed in high grade gliomas is shown to be derived from an increase in phosphocholine while the increase in the tCho peak detected in low grade gliomas is caused by augmented glycerophosphocholine content. The changes detected by ^{1}H HR-MAS are consistent with the upregulation of the choline kinase β or phospholipase C genes and the downregulation of the cytidyltransferase gene in high grade gliomas, or the upregulation of phospholipase A_1 detected in low grade gliomas.

EXPERIMENTAL

Tissue biopsies

Tumor specimens were provided by the Department of Neurosurgery, University Hospital 'La Paz', Madrid, complying with all bioethical criteria of the ethics committee of the Hospital. Tumor biopsies were obtained from the patients in the operating room following intracranial surgery, immediately frozen in liquid nitrogen and stored at −70°C until ^{1}H HR-MAS analysis. An adjacent biopsy of the tumor was obtained for histopathological classification. Tumor specimens from 23 patients were histologically classified according to the revised WHO criteria. The samples included nine low-grade astrocytomas (WHO grade II), six anaplastic astrocytomas (WHO grade III) and eight glioblastoma multiforme (WHO grade IV) (16). Grades III and IV were grouped as 'high grade' gliomas, to favour a more robust clinical classification between low and high grade gliomas. Normal brain samples ($n = 3$) were obtained from patients undergoing partial lobectomy as indicated in the treatment of some epilepsies (17).

Sample preparation for HR-MAS experiments

Before HR-MAS analysis, each sample (15–20 mg) was flushed with D_2O to remove the residual blood and water with the aim to improve water suppression. The sample was introduced in an HR-MAS zirconium rotor (4 mm OD) fitted with a 50 μl cylindrical insert to increase sample homogeneity and then transferred into the MAS probe, cooled to 4 °C. The HR-MAS spectra were acquired from a 11.7 Tesla MHz Bruker AVANCE Spectrometer operating at 500.13 MHz, at 4°C and 4 kHz spinning rate. 1D CPMG spectra were acquired using a water-suppressed spin-echo CPMG sequence with 5 s water presaturation during relaxation delay, 1 ms echo time (τ) and 144 ms total spin–spin relaxation delay ($2n\tau$), 32 786 data points and 128 scans (18). The 2D ^{1}H-COSY spectra were acquired using a gradient pulse sequence with 1 s water-presaturation during the relaxation delay, 4096 data points, 128 scans per increment and 256 increments (19).

Quantification

Quantification of tumor metabolites detectable in the *ex vivo* spectra was performed using the software program LCModel, a package for the automatic quantification of ^{1}H NMR spectra (Linear Combination of Model Spectra, http://s-provencher.com/pages/lcmodel.shtml (20)). The LCModel fits spectra as a linear combination of model spectra from 23 brain metabolites and optional contributions for lipids and macromolecules. For the analysis of our *ex vivo* data, a customized set of cerebral metabolites was prepared using the model solutions recommended by Dr S. Provencher including: alanine, lactate, taurine, phosphocreatine, creatine, choline, glycerophosphocholine, phosphorylethanolamine, phosphocholine, glycine, aspartic acid, glutamine, glutamate, *myo*-inositol, *N*-acetyl-aspartate, acetate, threonine, glutathione, valine, isoleucine, leucine, glucose and

GABA. The LCModel program found the best fit between the spectrum of the biopsy and the linear combination of the metabolite components, yielding values of metabolite content, with the fitting error expressed as the SD. Under these conditions, the concentrations of metabolites correspond to arbitrary units since the measurement of the absolute concentrations requires the system to be accurately calibrated with a precise knowledge of sample volume and weight (during rotation), a set of conditions difficult to fulfill in HR-MAS spectroscopy. To overcome this limitation, we used in the calculations relative concentrations to the total choline or creatine peaks. Only metabolite fittings with errors below 20% SD were included in the final analysis.

Sample preparation and analysis of individual gene expression assays

Total experimental RNA was prepared from biopsies of normal brain and tumors using the RNAspin Mini RNA Isolation kit (GE Healthcare). Approximately 20 mg biopsies were used. The purity and integrity of the labeled cRNA were evaluated from the A_{260}/A_{280} ratio on an Agilent 2100 bioanalyzer (Agilent Technologies Inc., Santa Clara, CA, USA), being always between 1.9–2.1. The RNA integrity number was evaluated using the Agilent 2100 bioanalyzer, assuming appropriate intensities as those depicting a 28S:18S ratio higher than 2. Values of the RNA integrity number (RIN) were normally $\geq$7. Approximately 250 ng of RNA were retrotranscribed to cDNA using the high capacity cDNA reverse transcription kit (Applied Biosystems, Foster City, CA, USA).

The expression of the genes of the choline pathway was assayed using the individual probes for each gene commercialized as TaqMan® (Applied Biosystems, Foster City, CA, USA). TaqMan® probes for gene expression provide one of the most comprehensive set of pre-designed real-time PCR assays available, including specifically most of the genes of the Kennedy pathway. All TaqMan® gene expression assays were run with the same real-time PCR protocol, eliminating the need for primer design or PCR optimization. Table 1 summarizes the transporters or enzymes of choline metabolism and the corresponding genes investigated in this study. The expression profiles of the different genes in tumor and healthy brain tissue were compared, assuming as a unit the value of the corresponding gene expression in the healthy brain.

Statistical analyses

The statistical analysis was performed using the SPSS package as implemented on a Windows XP Platform (SPSS Inc., Chicago, Illinois). Briefly, six variables were selected from the LCModel analysis and tested as possible classifiers to differentiate between low and high grade gliomas: Cho/tCho, GPC/tCho, PC/tCho, Cho/Cr, GPC/Cr and PC/Cr. In a first step, before any multivariate analysis, the different variables were tested for differences between low and high grade glioma by performing a simple *t*-test for each one individually. Then a classification analysis was implemented using a Logistic Regression (LR) algorithm. LR fits directly the probability of occurrence of a given condition for every biopsy (e.g. high Grade, p_H) based on a prediction function z containing the linear combination of variables X_j (Cho/tCho, GPC/tCho, PC/tCho, Cho/Cr, GPC/Cr, PC/Cr) and weighting parameters B_j (21,22).

$$\text{Probability of low Grade } p_H = \frac{e^Z}{1+e^Z} = \frac{1}{1+e^{-Z}} \quad (1)$$

$$Z = B_0 + B_1X_1 + B_2X_2 + \cdots + B_pX_p \ldots \quad (2)$$

The relationship between the variables X_j and p_H is nonlinear (eqn (1)), the corresponding parameters B_j being estimated using a

Table 1. Transporters or enzymes of choline metabolism and the corresponding genes

	Enzyme or transporter	Abbreviation	Gene name	Assay ID
1	Choline transporter		CTL1	Hs00223114_m1
			CTL2	Hs00220814_m1
2	Choline kinase	ckα	CHKA	Hs00608045_m1
	(EC 2.7.1.32)	ckβ	CHKB	Hs00193219_m1
3	Phosphocholine cytidylyltransferase	ctα	PCYT1A	Hs00192339_m1
	(EC 2.7.7.15)	ctβ	PCYT1B	Hs00191464_m1
4	Phosphocholine transferase	ptc	CHPT1	Hs00220348_m1
	(EC 2.7.8.2)			
5	Phospholipase D	plD1	PLD1	Hs00160118_m1
	(EC 3.1.4.4)	plD2	PLD2	Hs00160163_m1
6	Lysophospholipase	lpl	LYPLA1	Hs00272216_s1
	(EC 3.1.1.5)			
7	Glycerol-3-phosphate acyltransferases	at	GPAM	Hs00326039_m1
	(EC 2.3.1.15 and EC 2.3.1.51)			
8	Phospholipase C	plC	PLCG1	Hs00234046_m1
	(EC 3.1.4.3)			
10	Phospholipase A2	plA2 VI	PLA2G6	Hs00185926_m1
	(EC 3.1.1.4)	plA2 IV	PLA2G4A	Hs00233352_m1
11	Phospholipase A1	plA1	PLA1A	Hs00210729_m1
	(EC 3.1.1.32)			
12	Phosphatidate Phosphohydrolase	pap	PPAP2A	Hs00170356_m1
	(EC 3.1.3.4)			

maximal likelihood algorithm. To choose among the X_j variables those providing the best fit, we build the prediction function Z initially with all variables, eliminating variables progressively in a dichotomous manner, determining the weight of each removal in p_H as indicated by the corresponding B_j value. Larger B_j values indicate larger impact of the variable X_j on the model and consequently larger impact on the calculated probability. In the present work, the results of LR are expressed as the predicted probability of a given sample to be classified as a low grade glioma.

Materials

Metabolite standards were acquired from SIGMA (St.Louis, MO, USA) and were of the highest quality available. Deuterium oxide (99.9% ^{2}H), was obtained from Apollo Scientific (Bradbury, Stockport, UK).

RESULTS

Figure 1 shows representative ^{1}H HR-MAS 1D spectra of healthy brain (A), low and high grade gliomas (B and C), respectively. The main metabolites observed include: lactate (Lac), γ-amino butyric acid (GABA), of *N*-acetyl aspartate (NAA), glutamine and glutamate (Glx), creatine/phosphocreatine (Cr/PCr), Cho, GPC, PC, and *myo*-inositol (Myo). The broadened signals in the spectra originate from the presence of lipids and macromolecules (MM). A comparison between the glioma and the normal brain spectra shows the decrease, or absence, of the neuronal markers NAA and GABA and a progressive increase in the lipid content (see resonances *ca* 0.89 ppm), from low to high grade gliomas (23).

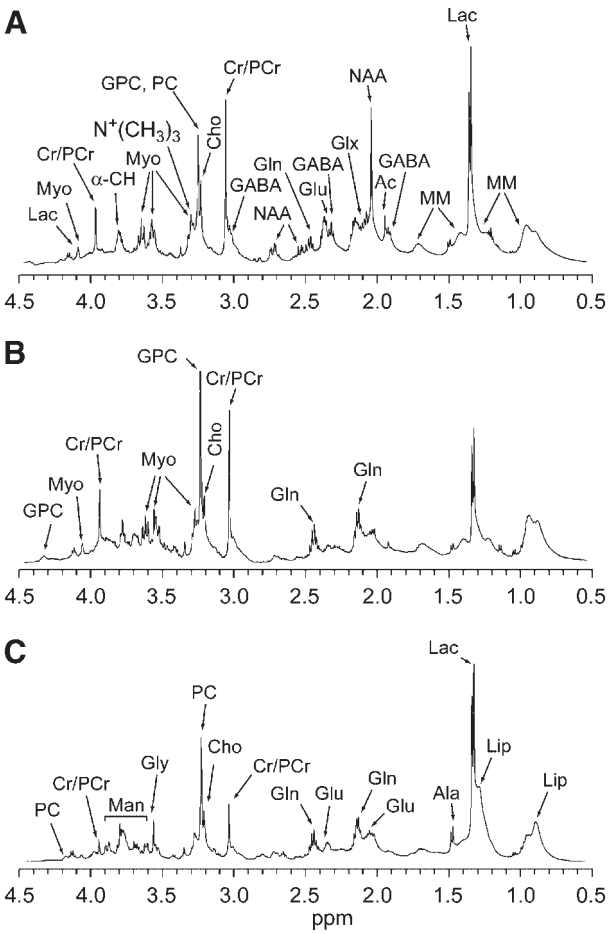

Figure 1. *Ex vivo* 1D water-presaturated ^{1}H HR-MAS NMR spectra: (A) healthy brain tissue, (B) low grade glioma, and (C) high grade glioma. Acquisition conditions were as indicated in the Experimental section. Ac, Acetate; Cho, choline; Cr/PCr, creatine/phosphocreatine; GABA, γ-amino butyric acid; Glx, glutamine plus glutamate; GPC, glycerophosphocholine; GPE, glycerophosphorylethanolamine; Lac, lactate; Lip, lipids; Man, mannitol; MM, macromolecules; Myo, *myo*-inositol; NAA, *N*-acetylaspartate; PC, phosphocholine.

The left panels of Fig. 2 depict representative metabolic profiles of healthy brain (A), low (B) and high (C) grade gliomas in the region from 3.0 to 4.4 ppm. The profiles illustrate well the improved spectral resolution obtained by the use of HR-MAS spectroscopy (CPMG, echo time 144 ms), as compared to *in vivo* spectra. Under these conditions, the broad resonances from lipids or macromolecules are attenuated and mainly low molecular weight metabolites become observable. The spectra show significant differences in the 3.22 ppm region containing the choline metabolites. The most noticeable difference between healthy and diseased tissue is the increased contribution of the Cho-containing metabolites, both in low and high grade gliomas. GPC appeared to be the main contributor to the total choline peak in low grade gliomas, whereas PC depicted the dominant contribution in high grade gliomas. A detailed inspection of the corresponding 2D COSY ^{1}H HR-MAS spectra (left panels) confirmed GPC as the dominant contributor to the total choline peak in low grade (3.67–4.33 ppm) and PC in the high grade gliomas (3.61–4.17 ppm crosspeak). Both correlations correspond to the scalar coupling between the methylene protons of the choline moiety in GPC and PC, respectively. It is interesting to note that the 2D HR-MAS approach allows the identification of additional metabolites like glycerolphosphorylethanolamine (GPE), taurine (Tau), and phosphoethanolamine (PE), not detectable in 1D spectra of the same biopsies. Interestingly, Manitol (Man, 3.68, 3.88 ppm-CH_2OH; 3.76 and 3.80 ppm-CHOH), a compound normally used during surgery of high grade gliomas to decrease cerebral edema, is clearly detected in many of these spectra. However, despite their advantages, the HR-MAS spectra shown provide only qualitative information on the contributions of choline containing metabolites in each tumor. In order to obtain a more quantitative interpretation, we adapted the LCModel approach, originally developed for *in vivo* spectroscopy (24), to the quantitative processing of ^{1}H HR-MAS spectra.

Figure 3 illustrates representative LCModel fits of HR-MAS spectra from a low (A) and high (B) grade glioma biopsy, respectively. The corresponding inserts show the expanded regions containing the choline and creatine resonances. The use of LCModel allows the correct quantification of the complete metabolite profile of the tumor, rather than providing isolated deconvolutions of specific resonances. This allows the optimal fit of partially overlapping resonances, such as those of PC, GPC, and free choline. In particular, the insert to Fig. 3A depicts more clearly the higher contribution of GPC to the total choline resonances, the PC contribution remaining very low. In this case, GPC content appears to reach the same intensity as the Cr/PCr composite resonance. The metabolic profile shown in the insert to Fig. 3B is clearly different, showing a dominant contribution of the PC peak with a virtually undetectable contribution of GPC. These different contributions of GPC and PC are also evident in the corresponding resonances of the –OCH_2– carbons at 4.33 and 4.17 ppm, respectively. In the high grade tumors, the combined Cr/PCr resonance is decreased.

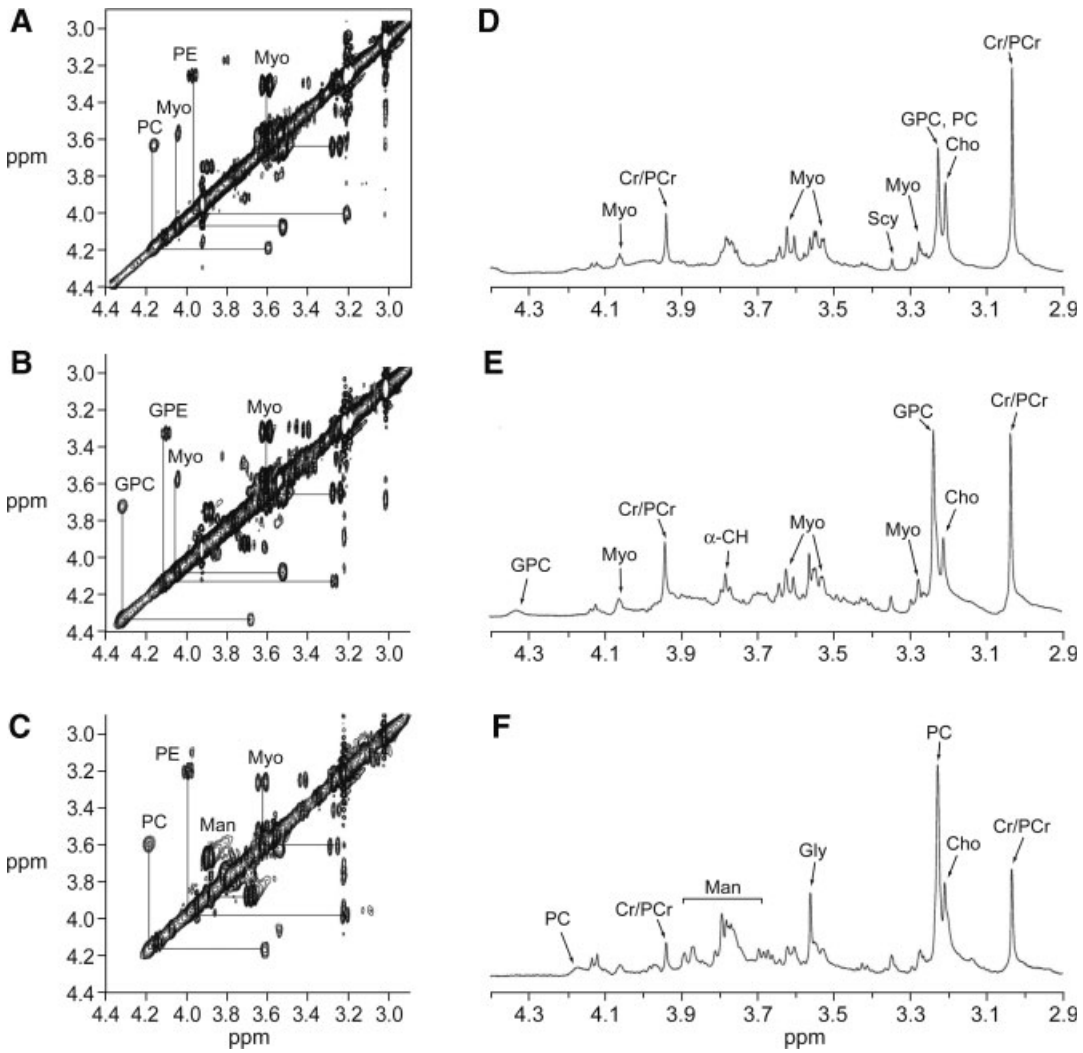

Figure 2. Left: partial COSY ^{1}H HR-MAS NMR spectra (3.0–4.4 ppm) of (A) healthy brain, (B) low grade glioma and (C) high grade glioma. Right: partial CPMG spectra (3.0–4.4 ppm) of (D) healthy brain, (E) low grade, and (F) high grade glioma. Note the characteristic correlations from GPC and PC in low grade and high grade gliomas. Acquisition conditions were as indicated in the Experimental section. Abbreviations are the same as those of Fig. 1.

Figure 4 summarizes the results obtained in the LCModel quantification of the relative ratios of free choline, PC and GPC to the total choline (upper panel) or to the total creatine (lower panel) resonance. The *t*-test shows that, while the choline to creatine ratio is not statistically different between low and high grade gliomas, ratios of both PC and GPC to total-choline exhibit statistically significant differences between the two tumor grades. In order to remove the uncertainties and improve the classification process we implemented the logistic regression (LR) analysis to investigate the optimal combination of variables to discriminate between high and low grade gliomas.

The variables tested were Cho/tCho, PC/tCho, GPC/tCho, Cho/Cr, PC/Cr, and GPC/Cr. From these, GPC/tCho showed the highest predictive score, closely followed by PC/tCho (data not shown). The combination of Cho/tCho, PC/tCho, and GPC/tCho allowed an unambiguous classification of all the tumors. However, because the use of three variables could be questioned considering the relatively small number of samples, we performed a similar LR analysis with just one variable, the one with the highest predictive score (GPC/tCho), and compared the results obtained with those provided by the tCho/Cr ratio (Table 2), normally used in *in vivo* spectroscopy (25). GPC/tCho allowed all the tumors, except for one, to be correctly discriminated between the low and high glioma grades (Table 2 and Fig. 5A), whereas tCho/Cr yielded significantly worse classification results (Table 2 and Fig. 5B).

Figure 6 depicts the expression of the genes of choline metabolism in high grade (light grey) and low grade (dark grey) glioma biopsies relative to the expression found in normal brain. Ratios with values higher or lower than unity reveal upregulation or downregulation of the corresponding gene as compared to its expression in the normal brain. In high grade gliomas, the following genes were found to be upregulated: choline transporter (CTL2), choline kinase (CHKB), phospholipases A, C, and D (PLA2G4A, PLCG1, and PLD2) and lysophospholipase (LYPLA1), the upregulation being significant in phospholipases A and C. The remaining genes investigated in high grade gliomas were downregulated. In the low grade gliomas, the upregulated genes were: choline transport (CTL1, CTL2), cytidylyl-transferase (PCYT1A, PCYT1B), phospholipases A and D (PLA2G4A, PLA1A, and PLD2) and lysophospholipase (LYPLA1), the remaining being downregulated. Notably, some genes were upregulated in high grade gliomas and downregulated in low grade gliomas, like

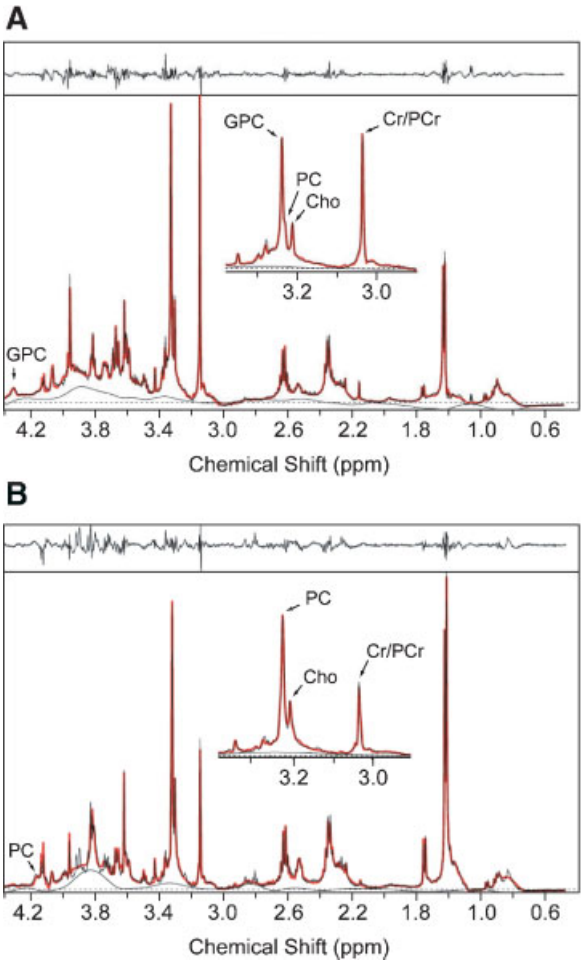

Figure 3. LCModel fits of ^{1}H CPMG HRMAS spectra acquired from representative low grade (A) and high grade (B) gliomas. The top panels show the difference between the spectrum obtained from the biopsy (black) and the LCModel simulated spectrum (red) obtained using the metabolite dataset prepared in our laboratory.

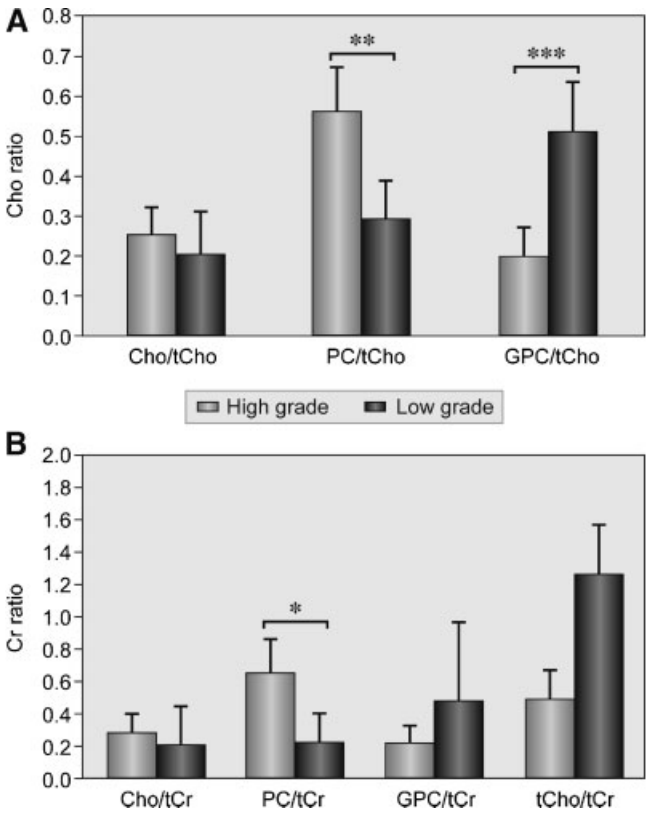

Figure 4. Relative contributions of Cho, PC and GPC with respect to tCho (A) and to tCr (B) in high grade (light grey) and low grade (dark grey) gliomas. $^*p < 0.05$, $^{**}p < 0.005$, $^{***}p < 0.001$. The values correspond to the arithmetic mean and the error bars to the standard deviation of the mean.

choline kinase (CHKB) and phospholipase C (PLCG1), while others were upregulated in low grade gliomas and downregulated in high grade gliomas, like the choline transporter (CTL1), citydyltransferase (PCYT1B) and phospholipase A (PLA1A). Of these, only the differences in phospholipase C (PLCG1) upregulation and downregulation between high grade and low grade gliomas, became statistically significant. In general, high grade gliomas depicted significantly upregulated phospholipase A_2 and C expression as compared to low grade gliomas.

DISCUSSION

The present work illustrates how *ex vivo* ^{1}H HR-MAS analysis of tissue biopsies can help the discrimination of high grade and low grade human astrocytomas, through the quantitative investigation of the metabolic profile of choline containing metabolites. Previous studies have used ^{1}H HR-MAS to investigate the complete metabolic profile of cerebral tumors (11,13,26). These initial studies described the methodology and provided the assignments, but the spectral information remained at the qualitative level without the implementation of multivariate statistical methodologies. In general, the analysis of the resonances from choline containing compounds remained limited, since they overlapped to some extent and it was not possible to provide accurate quantification values without the use of more elaborate spectral deconvolution algorithms.

Our approach overcomes this limitation by implementing a robust procedure for the quantification of the different choline

Table 2. Classification of human glioma grade by logistic regression

X_j	B_j (S.E.)	Significance	B_0 (S.E.)	Significance
GPC/tCho	22.908 (11.617)	0.049	−7.022 (3.458)	0.042
tCho/Cr	−0.561 (0.745)	0.451	0.852 (0.948)	0.369

B_j indicates the fitted value of the parameter corresponding to the X_j variable in eqn (2). B_0 is the constant term in eqn 2. The classification results corresponding to these two equations are plotted in Fig. 5. Abbreviations are the same as those of Fig. 1.

NMR IN BIOMEDICINE

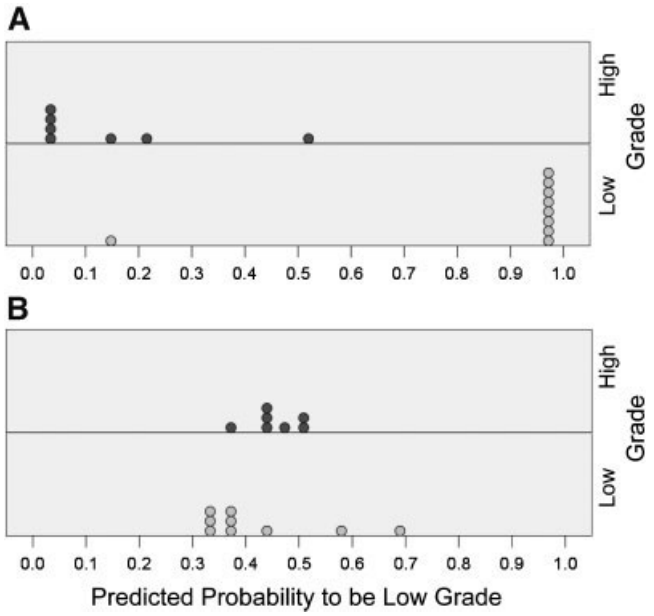

Figure 5. Predicted probabilities obtained from the LR analysis in the classification of high (dark grey circles) and low grade (light grey circles) gliomas using the GPC/tCho ratio (A) and tCho/Cr ratio (B) as variables. For a given biopsy, a probability of 1 indicates unambiguous classification as low grade glioma and a probability of 0 its unambiguous classification as high grade glioma. Intermediate values correspond to different levels of uncertainty. Note that the classifier used in (A) provides a correct value in all cases except one while the classifier used in (B) provides very poor classification.

containing metabolites in ^{1}H HR-MAS spectra using the LCModel approach. LCModel allows the relative quantification of the complete metabolite profile of the biopsy. In this work, we used a database containing the spectra of 23 cerebral metabolites to calculate the corresponding linear combination that would optimally fit the experimental spectrum. In this study, we focus only on the profile of choline containing metabolites. Relative quantifications performed *in vivo* (10) have shown that the total choline peak to creatine ratio is increased in both low and high grade gliomas and that there is a significant correlation between tCho levels and glioma malignancy. However, the absolute quantification of tumor metabolites led to some contradictory

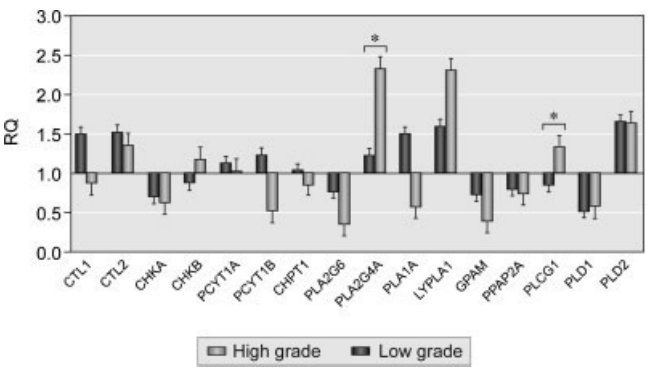

Figure 6. Relative expression (RQ) of the genes of the Choline Cycle in low grade (dark grey) and high grade (light grey) gliomas as compared to the normal brain. RQ>1 indicates upregulation and RQ<1 reveals down-regulation, as compared to healthy brain RQ = 1. $^*p < 0.05$. Abbreviations are the same as those of Table 1.

results. Several authors (27–30) reported higher concentrations of Cho-containing compounds in extracts of high grade than in low grade gliomas, while Usenius *et al*. (31) did not find significant differences in tCho among the different glioma grades. Nevertheless, both Usenius *et al*. (31) and Sabatier *et al*. (30) reported alterations in the relative contribution of the different Cho-containing compounds to the tCho peak in tumor extracts. The latter results are in agreement with our present ^{1}H HR-MAS findings. We show here that the relative contribution of phosphocholine to the total choline peak is higher in high grade gliomas while the relative contribution of glycerophosphocholine dominates the total choline peak in low grade gliomas. This allows a convenient and fast discrimination of high grade and low grade gliomas by ^{1}H HR MAS spectroscopy.

An important aspect of the present study is the genetic basis of the metabolite alterations observed by ^{1}H HR-MAS. Although the metabolic phenotype or metabolome cannot be strictly considered as a direct expression of the genome, since post-transcriptional events may modulate the ultimate genomic expression, our results suggest that both events appear to be tightly connected in human gliomas. Two studies have previously addressed this aspect (15,32): Griffin *et al*. used high resolution ^{1}H NMR spectra of body fluids to investigate the global system dynamics in drug metabolism and its disturbances (32) and Tzika *et al*. investigated the relationship between HR-MAS spectra of tumor biopsies and the complete genome analysis (15,32). Much less information is available on the relative expression of the genes of the Kennedy pathway and the pattern of choline metabolites as detected by ^{1}H HR-MAS.

Figure 7 provides an adequate frame to discuss these aspects, by showing in more detail the metabolism of choline phospholipids, the enzymes involved and the different genes coding for them (*ck,* choline kinase; *ct,* cytidylyl-transferase; *ptc,* phosphocholine cytidylyl-transferase; *pla,* phospholipase A_1 and A_2; *lpl,* lysophospholipase; *pd,* glycerophosphocholine phosphodiesterase; *at*, glycerol-3-phosphate acyltransferases; *plc,* phospholipase C; *pld,* phospholipase D).

Modern gene expression technologies allow us to investigate specifically the genes of a specific pathway, rather than the complete genome as previously done. In this work, we investigated the individual expression of 16 genes of choline metabolism, to improve our understanding of the genetic basis of the metabolic profile observed by ^{1}H HR-MAS. Particularly interesting are those changes in genetic expression corresponding to genes depicting a crossover, becoming upregulated in one type of gliomas and downregulated in the other.

The increase in PC in high grade gliomas can be explained by the increase in the expression of the choline kinase β gene and the phospholipase C gene, respectively. Several authors have described increases in the expression of the genes of choline transport (33) and choline kinase (34,35). Choline kinase activity is coded by the α and β genes which give rise to three homodimeric (αα, ββ) or heterodimeric (αβ) isoforms of the enzyme (34,35). Present results parallel previous observations, suggesting that the genes coding for the choline transporter β or the β isoforms of choline kinase, are the ones responsible for the increase in PC in human gliomas. In addition, we show that there are significant increases in the expression of the phospholipase C gene in high grade gliomas, another potential source of PC. This is, to our knowledge a novel finding, indicating that the increase in PC is derived not only from an increase in its synthesis by choline kinase but by an increased degradation of phosphatidylcholine through the phospholipase C pathway. Together,

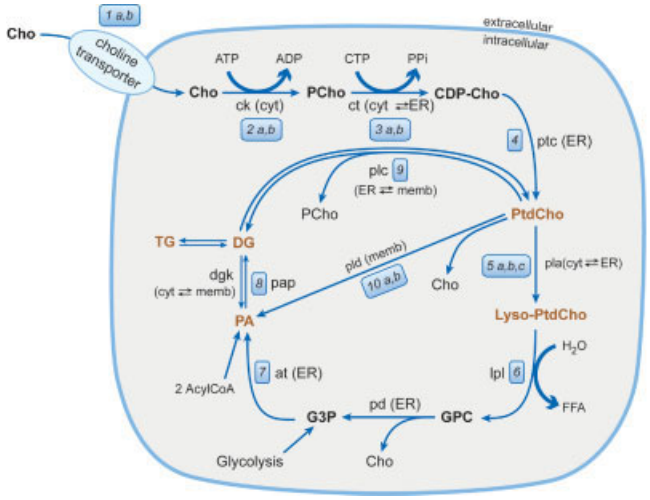

Figure 7. The Kennedy pathway of phosphatidylcholine metabolism. Metabolites: *Cho,* choline; *PCho,* phosphocholine; *CDP-Cho,* cytidin diphosphate choline; *PtdCho*, Phosphatidylcholine; *Lyso-PtdCho*, 1-acyl or 2-acyl phosphatidylcholine; *GPC,* glycerophosphocholine; *G3P, sn*-glycerol-3-phosphate; *PA,* phosphatidate; *DG,* diacylglycerol; *TG,* triacylglycerol. Enzymes: *ck,* choline kinase (2 a,b); *ct,* cytidylyl-transferase (3 a,b); *ptc,* phosphocholine cytidylyl-transferase (4); *pla,* phospholipase A_1 and phospholipase A_2 (5 a,b,c); *lpl,* lysophospholipase (6); *pd,* glycerophosphocholine phosphodiesterase; *at*, glycerol-3-phosphate acyltransferases (7); *plc,* phospholipase C (9); *pld,* phospholipase D (10). Cellular compartments: ER, endoplasmatic reticulum; cyt, cytosol; memb, membrane.

these results suggest an increase in the turnover rate of phosphatidylcholine with glioma grade. Moreover, some cancer therapies have proposed the use of choline kinase inhibitors (34,36). Present results indicate that the additional inhibition of the phospholipase C pathway may provide a useful complement to these therapies.

The increase in GPC in the low grade gliomas reflects a positive balance between its production and degradation pathways. Net GPC synthesis is favoured by the increased relative expression of the choline transporter gene (α), cytidylyl-transferase gene (β), and the phospholipases A1 (PLA1) and A2 (PLA2), respectively. PLA1 is increased in low grade and decreased in high grade gliomas favoring GPC accumulation in the low grade gliomas (37). PLA2 is encoded by a family of 14 different genes, including the PLA2G4A and PLA2G6 genes investigated here (38). No significant differences were found between low and high grade gliomas in the expression of the PLD1 or PLD2 genes, coding for phospholipase D catalyzed GPC degradation. Our results suggest that the increases in PLA1 combined with a positive balance in the combined expression of PLA2G6 and PLA2G4A contribute to the observed increase in GPCs in low grade gliomas. Furthermore, the relative amount of GPC to PC in low grade gliomas may be favourable to the former, because of the reduced expression of the phospholipase C gene in low grade tumors. In other words, the net balance between increased synthesis, reduced degradation, and decreased PC synthesis through phospholipase C, may lead ultimately to relative GPC accumulation in low grade gliomas. This is an interesting finding since only one previous study to our knowledge, reported on the genes regulating GPC metabolism in mammary tumors (39).

In summary, we provided a pilot investigation on the application of ^{1}H HR-MAS spectroscopy to the classification of human glioma biopsies. Our results show that high and low grade gliomas are characterized by increases in PC or GPC, respectively, and that these appear to be reflected by changes in the expression of the genes of the Kennedy pathway of choline metabolism.

Acknowledgements

This study was supported in part by grants from the Spanish Ministry of Education and Science SAF 2004–03197 and NAN 2004–09125-C07–03, grant S-BIO/0179/2006 from the Community of Madrid and the Integrated EU Project MEDITRANS (Contract No 026668) to S.C., grant PI051845 from the Institute of Health Charles III to M.L.G.M., grant IT0725H5F4 from the Italian Government to L.S. and Acción Integrada Hispano-Italiana HI2006–0101 to L.S. and S.C. We are indebted to Dr J. Alonso for the total RNA extraction, and to Dr S. Provencher for excellent advise in the implementation of the LCModel program for HR MAS. V.R. holds a predoctoral fellowship from the Italian Ministry of Education and Science.

REFERENCES

1. Galanaud D, Chinot O, Metellus P, Cozzone P. [Magnetic resonance spectroscopy in gliomas] (in French). Bull. Cancer 2005; 92(4): 327–331.
2. Lafuente JV, Alkiza K, Garibi JM, Alvarez A, Bilbao J, Figols J, Cruz-Sanchez FF. Biologic parameters that correlate with the prognosis of human gliomas. Neuropathology 2000; 20(3): 176–183.
3. Narayana A, Chang J, Thakur S, Huang W, Karimi S, Hou B, Kowalski A, Perera G, Holodny A, Gutin PH. Use of MR spectroscopy and functional imaging in the treatment planning of gliomas. Br. J. Radiol. 2007; 80(953): 347–354.
4. Negendank WG, Sauter R, Brown TR, Evelhoch JL, Falini A, Gotsis ED, Heerschap A, Kamada K, Lee BC, Mengeot MM, Moser E, Padavic-Shaller KA, Sanders JA, Spraggins TA, Stillman AE, Terwey B, Vogl TJ, Wicklow K, Zimmerman RA. Proton magnetic resonance spectroscopy in patients with glial tumors: a multicenter study. J. Neurosurg. 1996; 84(3): 449–458.
5. Chen CY, Lirng JF, Chan WP, Fang CL. Proton magnetic resonance spectroscopy-guided biopsy for cerebral glial tumors. J. Formos. Med. Assoc. 2004; 103(6): 448–458.
6. McKnight TR, Lamborn KR, Love TD, Berger MS, Chang S, Dillon WP, Bollen A, Nelson SJ. Correlation of magnetic resonance spectroscopic and growth characteristics within Grades II and III gliomas. J. Neurosurg. 2007; 106(4): 660–666.
7. Yerli H, Agildere AM, Ozen O, Geyik E, Atalay B, Elhan AH. Evaluation of cerebral glioma grade by using normal side creatine as an internal reference in multi-voxel 1H-MR spectroscopy. Diagn. Interv. Radiol. 2007; 13(1): 3–9.
8. McKnight TR. Proton magnetic resonance spectroscopic evaluation of brain tumor metabolism. Semin. Oncol. 2004; 31(5): 605–617.
9. Daly PF, Lyon RC, Faustino PJ, Cohen JS. Phospholipid metabolism in cancer cells monitored by 31P NMR spectroscopy. J. Biol. Chem. 1987; 262(31): 14875–14878.
10. Jeun SS, Kim MC, Kim BS, Lee JM, Chung ST, Oh CH, Lee SY, Choe BY. Assessment of malignancy in gliomas by 3T 1H MR spectroscopy. Clin. Imaging 2005; 29(1): 10–15.
11. Cheng LL, Chang IW, Louis DN, Gonzalez RG. Correlation of high-resolution magic angle spinning proton magnetic resonance spectroscopy with histopathology of intact human brain tumor specimens. Cancer Res. 1998; 58(9): 1825–1832.
12. Tzika AA, Cheng LL, Goumnerova L, Madsen JR, Zurakowski D, Astrakas LG, Zarifi MK, Scott RM, Anthony DC, Gonzalez RG, Black PM. Biochemical characterization of pediatric brain tumors by using

in vivo and ex vivo magnetic resonance spectroscopy. J. Neurosurg. 2002; 96(6): 1023–1031.
13. Martinez-Bisbal MC, Marti-Bonmati L, Piquer J, Revert A, Ferrer P, Llacer JL, Piotto M, Assemat O, Celda B. 1H and 13C HR-MAS spectroscopy of intact biopsy samples ex vivo and *in vivo* 1H MRS study of human high grade gliomas. NMR Biomed. 2004; 17(4): 191–205.
14. Valonen PK, Griffin JL, Lehtimaki KK, Liimatainen T, Nicholson JK, Grohn OH, Kauppinen RA. High-resolution magic-angle-spinning 1H NMR spectroscopy reveals different responses in choline-containing metabolites upon gene therapy-induced programmed cell death in rat brain glioma. NMR Biomed. 2005; 18(4): 252–259.
15. Tzika AA, Astrakas L, Cao H, Mintzopoulos D, Andronesi OC, Mindrinos M, Zhang J, Rahme LG, Blekas KD, Likas AC, Galatsanos NP, Carroll RS, Black PM. Combination of high-resolution magic angle spinning proton magnetic resonance spectroscopy and microscale genomics to type brain tumor biopsies. Int. J. Mol. Med. 2007; 20(2): 199–208.
16. Biernat W. 2000 World Health Organization classification of tumors of the nervous system. Pol. J. Pathol. 2000; 51(3): 107–114.
17. Pascual JM, Carceller F, Cerdán S, Roda JM. Diagnóstico diferencial de tumores cerebrales '*in vitro*' por espectroscopía de resonancia magnética de protón. Método de los cocientes espectrales. Neurocirugía 1998; 9: 4–10.
18. Meiboom S, Gill D. Modified spin-echo method for measuring nuclear relaxation time. Rev. Sci. Instrum. 1958; 29: 688–691.
19. Aue WP, Bartholdi E, Ernst RR. Two-dimensional spectroscopy: application to nuclear magnetic resonance. J. Chem. Phys. 1976; 64: 2229–2246.
20. Provencher SW. Estimation of metabolite concentrations from localized *in vivo* proton NMR spectra. Magn. Reson. Med. 1993; 30(6): 672–679.
21. Agresti A. *Categorical Data Analysis*, 2nd (ed). John Wiley and Sons, Inc.: New York, 2002.
22. Tatsuoka M. *Multivariate analysis*. John Wiley & Sons, Inc.: New York, 1971.
23. Opstad KS, Bell BA, Griffiths JR, Howe FA. An investigation of human brain tumour lipids by high-resolution magic angle spinning (1)H MRS and histological analysis. NMR Biomed. 2008.
24. Kanowski M, Kaufmann J, Braun J, Bernarding J, Tempelmann C. Quantitation of simulated short echo time 1H human brain spectra by LCModel and AMARES. Magn. Reson. Med. 2004; 51(5): 904–912.
25. Kim JH, Chang KH, Na DG, Song IC, Kwon BJ, Han MH, Kim K. 3T 1H-MR spectroscopy in grading of cerebral gliomas: comparison of short and intermediate echo time sequences. AJNR Am. J. Neuroradiol. 2006; 27(7): 1412–1418.
26. Martinez-Bisbal MC, Celda-Munoz B, Marti-Bonmati L, Ferrer-Ripolles P, Revert-Ventura AJ, Piquer-Belloch J, Molla-Olmos E, Arana-Fernandez de Moya E, Dosda-Munoz R. [The contribution of magnetic resonance spectroscopy to the classification of high grade gliomas. The predictive value of macromolecules]. Rev. Neurol. 2002; 34(4): 309–313.
27. Kinoshita Y, Kajiwara H, Yokota A, Koga Y. Proton magnetic resonance spectroscopy of brain tumors: an *in vitro* study. Neurosurgery 1994; 35(4): 606–613; discussion 613-614.
28. Kinoshita Y, Yokota A. Absolute concentrations of metabolites in human brain tumors using *in vitro* proton magnetic resonance spectroscopy. NMR Biomed. 1997; 10 2–12.
29. Peeling J. Sutherland G. High-resolution 1H NMR spectroscopy studies of extracts of human cerebral neoplasms. Magn. Reson. Med. 1992; 24(1): 123–136.
30. Sabatier J, Gilard V, Malet-Martino M, Ranjeva JP, Terral C, Breil S, Delisle MB, Manelfe C, Tremoulet M, Berry I. Characterization of choline compounds with *in vitro* 1H magnetic resonance spectroscopy for the discrimination of primary brain tumors. Invest. Radiol. 1999; 34(3): 230–235.
31. Usenius JP, Vainio P, Hernesniemi J, Kauppinen RA. Choline-containing compounds in human astrocytomas studied by 1H NMR spectroscopy *in vivo* and *in vitro*. J. Neurochem. 1994; 63(4): 1538–1543.
32. Griffin JL, Scott J, Nicholson JK. The influence of pharmacogenetics on fatty liver disease in the wistar and kyoto rats: a combined transcriptomic and metabonomic study. J. Proteome Res. 2007; 6(1): 54–61.
33. Aboagye EO, Bhujwalla ZM. Malignant transformation alters membrane choline phospholipid metabolism of human mammary epithelial cells. Cancer Res. 1999; 59(1): 80–84.
34. Glunde K, Bhujwalla ZM. Choline kinase alpha in cancer prognosis and treatment. Lancet Oncol. 2007; 8(10): 855–857.
35. Mori N, Glunde K, Takagi T, Raman V, Bhujwalla ZM. Choline kinase down-regulation increases the effect of 5-fluorouracil in breast cancer cells. Cancer Res. 2007; 67(23): 11284–11290.
36. Hernandez-Alcoceba R, Fernandez F, Lacal JC. *In vivo* antitumor activity of choline kinase inhibitors: a novel target for anticancer drug discovery. Cancer Res. 1999; 59(13): 3112–3118.
37. Hiramatsu T, Sonoda H, Takanezawa Y, Morikawa R, Ishida M, Kasahara K, Sanai Y, Taguchi R, Aoki J, Arai H. Biochemical and molecular characterization of two phosphatidic acid-selective phospholipase A1s, mPA-PLA1alpha and mPA-PLA1beta. J. Biol. Chem. 2003; 278(49): 49438–49447.
38. Cummings BS. Phospholipase A2 as targets for anti-cancer drugs. Biochem. Pharmacol. 2007; 74(7): 949–959.
39. Glunde K, Jie C, Bhujwalla ZM. Molecular causes of the aberrant choline phospholipid metabolism in breast cancer. Cancer Res. 2004; 64(12): 4270–4276.

